

Dalton Transactions

Accepted Manuscript



This is an *Accepted Manuscript*, which has been through the Royal Society of Chemistry peer review process and has been accepted for publication.

Accepted Manuscripts are published online shortly after acceptance, before technical editing, formatting and proof reading. Using this free service, authors can make their results available to the community, in citable form, before we publish the edited article. We will replace this *Accepted Manuscript* with the edited and formatted *Advance Article* as soon as it is available.

You can find more information about *Accepted Manuscripts* in the [Information for Authors](#).

Please note that technical editing may introduce minor changes to the text and/or graphics, which may alter content. The journal's standard [Terms & Conditions](#) and the [Ethical guidelines](#) still apply. In no event shall the Royal Society of Chemistry be held responsible for any errors or omissions in this *Accepted Manuscript* or any consequences arising from the use of any information it contains.

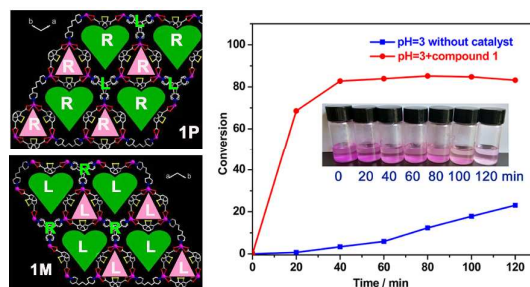
Syntheses, structures, photoluminescence and photocatalysis of chiral 3D Cd(II) frameworks from achiral mixed flexible ligands by spontaneous resolution

Yan-Qiong Sun,^{*a,b} Jie-Cen Zhong,^a Ling Ding^a and Yi-Ping Chen^a

College of Chemistry, Fuzhou University, Fuzhou, Fujian 350108, People's Republic of China. Fax: +86-591-22866340; E-mail sunyq@fzu.edu.cn

^b State Key Laboratory of Structural Chemistry, Fujian Institute of Research on the Structure of Matter, Chinese Academy of Sciences, Fuzhou, Fujian 350002, PR China

Two three-interpenetrating chiral cadmium MOF enantiomers with good photocatalytic activities for degradation of dye were constructed from achiral flexible ligands.



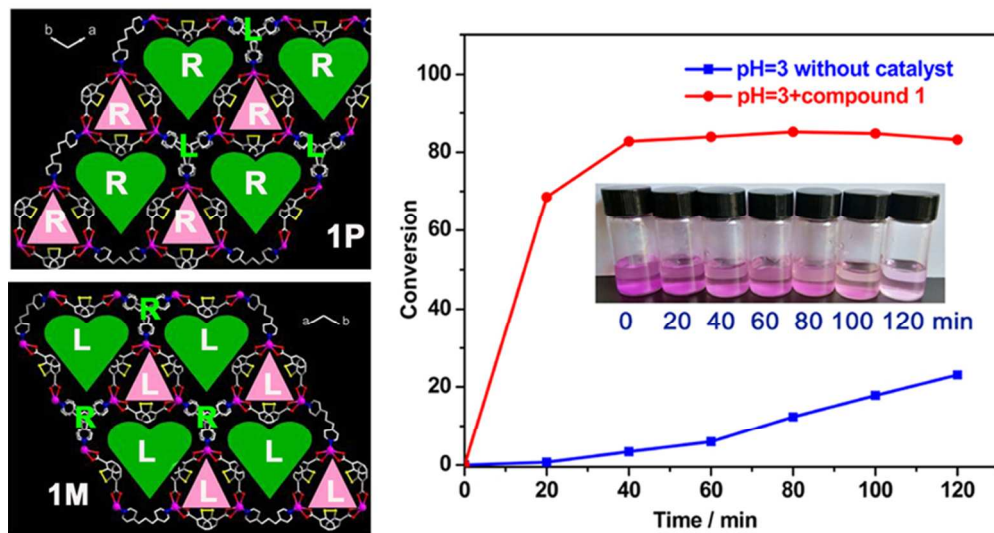


Figure Abstract
75x39mm (300 x 300 DPI)

Syntheses, structures, photoluminescence and photocatalysis of chiral 3D Cd(II) frameworks from achiral mixed flexible ligands by spontaneous resolution

Cite this: DOI: 10.1039/x0xx00000x

Received 00th January 2012,
Accepted 00th January 2012

DOI: 10.1039/x0xx00000x

www.rsc.org/

Yan-Qiong Sun,^{*a,b} Jie-Cen Zhong,^a Ling Ding^a and Yi-Ping Chen^a

Unprecedented two homochiral Cd(II) enantiomers [Cd(dtba)(bpp)]_n (**1**: **1P** and **1M**) (H₂dtba=2,2'-dithiodibenzoic acid, bpp=1,3-bis(4-pyridyl)propane), were obtained by self-assembly with mixed achiral flexible ligands. Single-crystal X-ray diffraction analysis reveals that complexes **1P** and **1M** crystallize in trigonal space group P3₁21 and P3₂21, respectively. The compounds are optically active, and their UV spectra in the solid state showed Cotton effects in the opposite direction. Compounds **1P** and **1M** present the examples of three-interpenetrating chiral frameworks with triangular and quasi-heart-like threefold helical chiral channels, chair-like twofold helical chiral channels and one kind of threefold double-helical chain. The 3D metal-organic framework can be regarded as a *bcu*-type topology with the symbol of 8⁶. The photoluminescent property of compound **1** has been studied. Remarkably, Compound **1** exhibits good photocatalytic activity for degradation of dye under the simulated sunlight irradiation in the pH = 3 aqueous solution.

Introduction

Helical structures through self-assembly are necessary to our life and are of interest in recent research due to their novel chiral structures.¹⁻² So the designs and syntheses of chiral complexes are of particular attention owing to their potential applications in enantioselective separation³⁻⁴ and asymmetric catalysis.⁵⁻⁶ To best of our knowledge, there are three methods to obtain the chiral complexes: (1) Stereoselective syntheses using enantiopure organic ligands.⁷ With this method, the absolute configuration of the chiral complexes can be predetermined and the product crystals would be homochiral. (2) Chiral syntheses using chiral auxiliaries such as chiral solvents, catalysts or templates to a particular handedness.⁸ (3) Spontaneous resolution upon crystallization without any chiral auxiliaries.^[9-10] A spontaneous resolution phenomenon is observed for a certain kind of racemic mixed crystals comprised of equal amount of enantiomers with opposite chirality. A large number of examples of chiral spontaneous resolution were reported.^[11-12] However, so far, spontaneous resolution without any chiral auxiliaries is hard to predict

because the laws of physical determining the processes are not yet fully understood. Therefore, it is difficult to control the spontaneous resolution process owing to the discriminative interactions influencing the chirality resolution. Generally, the chirally discriminative interactions may arise from coordination bonds, hydrogen bonds, or π - π packing interactions due to their strong, selective and direction natures. In most instances of spontaneous resolution, chirality results from the coordination of the achiral ligands with the metal ions to form helical chains running along the screw axis. The achiral organic ligands with flexible conformations and skew coordination orientations are favorable for constructing a helical structure.

Along these lines, we chose the long flexible ligands of 2,2'-dithiodibenzoic acid (H₂dtba) and 1,3-bis(4-pyridyl)propane (bpp) to construct chiral coordination polymers based on the following consideration: (1) The twisted conformations of H₂dtba and bpp ligands provide the potential capability to form helical structures. The rotatable C-S, S-S single bonds in H₂dtba ligand and C-C bonds in bpp ligand enable the ligands to have flexible conformational adaptations (Fig.S1).^[13-15] (2) Their axial chirality potentially generates M and P enantiomers.^[16] The flexible 1,3-bis(4-pyridyl)propane ligand (bpp) with trimethylene part can supply a variety of conformations (TT, TG, GG and GG', where T = trans and G = gauche) (Fig.S2), which display quite different N-N distances and bend angles.^[17] (3) The skew coordination orientation of the carboxyl groups in H₂dtba ligand is favorable for

^a College of Chemistry, Fuzhou University, Fuzhou, Fujian 350108, People's Republic of China. Fax: +86-591-22866340; E-mail sunyq@fzu.edu.cn

^b State Key Laboratory of Structural Chemistry, Fujian Institute of Research on the Structure of Matter, Chinese Academy of Sciences, Fuzhou, Fujian 350002, PR China

† Electronic Supplementary Information (ESI) available: supplementary 14 plots including structures, luminescent spectra, XPRD, TG and FT-IR. See DOI: 10.1039/b000000x.

constructing a helical structure, which has been well documented in metal carboxylates.^[18]

In this paper, we report two homochiral enantiomers [Cd(dtba)(bpb)]_n (**1P** and **1M**), which are resolved by spontaneous resolution upon crystallization, in the absence of any chiral sources into 3D chiral metal-organic frameworks. Compounds **1P** and **1M** consist of three-fold [Cd(dtba)]_n single helical chains and three-fold [Cd(bpb)]_n double helical chains. Interestingly, the helical chirality handedness can influence the complexes **1P** and **1M** to induce P₃₁ and P₃₂ helical chains, respectively. Furthermore, the chiral compounds were characterized with solid-state circular dichroism (CD) spectra and fluorescence spectra. Compound **1** (**1P** and **1M**) is found to be able to photocatalytically degrade Rhodamine-B in the pH = 3 aqueous solution in a relatively efficient way.

Experimental section

General information

Commercially available solvents and chemicals were used without further purification. IR spectra were measured as KBr pellets on a Perkin-Elmer Spectrum 2000 FT-IR in the range 400-4000 cm⁻¹. The powder XRD patterns were recorded on a PANalytical X'pert Pro diffractometer equipped with Co K α radiation ($\lambda = 1.78901 \text{ \AA}$) at room temperature. The C, H and N elemental analyses were performed with an Elementar Vario EL III elemental analyzer. Thermogravimetric data was collected on a Mettler Toledo TGA/SDTA 851^e analyzer in flowing nitrogen at a heating rate of 10 °C/min. Luminescence measurements were made with an Edinburgh Instrument FS920 TCSPC luminescence spectrometer on powder crystal material of the compounds. CD spectra were recorded in a MOS-450 spectrophotometer, the scan rate was 500 nm/min, and all of the spectra were accumulated two times.

Photocatalytic activities of the prepared samples were evaluated by the degradation of RhB (10 mg/L) under simulated irradiation. A 300 W Xenon lamp was used as a light source. Before the irradiation, the compound **1** as photocatalyst was dispersed in the solution by magnetically stirring in the dark for about 2h to reach an adsorption/desorption equilibrium between the photocatalysts and RhB. Then, the suspensions were exposed to simulated sunlight irradiation. About 3 mL of suspension was sampled every 20 min and centrifuged to separate the photocatalyst. The filtrate was analyzed by using a UV-vis spectrophotometer (Shimadzu UV1750), and the concentration of RhB was monitored at 554 nm.

Synthesis of compounds

[Cd(dtba)_{0.5}(bpb)_{0.5}]_n 2,2'-Dithiodibenzoic acid (0.090 g, 0.3 mmol), 1,3-bis(4-pyridyl)propane (0.040 g, 0.2 mmol) and CdO (0.025 g, 0.2 mmol) were dissolved in 5 ml DMF. After being stirred for 30 mins, The aqueous solution was sealed in 25 ml Parr Teflon-lined stainless steel auto-clave and heated at 80 °C for 2d and then cooled to the room temperature for 1d. Brown block crystals suitable for X-ray analysis were obtained in 70% yield on cadmium basis. Anal. Calc for C₂₇H₂₂CdN₂O₄S₂: C,

52.37; H, 3.61; N, 4.52 wt%; Found: C, 52.68; H, 3.58; N, 4.56 wt%. The IR data (KBr, cm⁻¹): 3060(w), 1650(s), 1573(s), 1458(s), 1398(s), 1282(m), 1036(m), 860(m), 746(s), 478(m) (Fig.S3).

Table 1. Crystal data and structure refinement for **1**

Compound	1P	1M
Formula	C ₂₇ H ₂₂ CdN ₂ O ₄ S ₂	C ₂₇ H ₂₂ CdN ₂ O ₄ S ₂
<i>M_r</i> (g. mol ⁻¹)	614.99	614.99
Crystal system	trigonal	trigonal
space group	<i>P</i> ₃₁ <i>21</i>	<i>P</i> ₃₂ <i>21</i>
<i>a</i> (Å)	11.5660(10)	11.684(4)
<i>b</i> (Å)	11.5660(10)	11.684(4)
<i>c</i> (Å)	16.035(3)	16.157(8)
α (°)	90	90
β (°)	90	90
γ (°)	120	120
<i>V</i> (Å ³)	1857.7(4)	1910.1(17)
<i>Z</i>	3	3
<i>D_c</i> (g/cm ³)	1.649	1.608
μ (mm ⁻¹)	1.088	1.058
Flack parameter	0.15(2)	-0.02(3)
reflns collected/ unique	12954/ 2224	18332/2914
<i>R_{int}</i>	0.0523	0.1174
θ range/deg	2.03-25.29	3.23-27.48
<i>F</i> (000)	936	935
GOOF on <i>F</i> ²	1.076	1.215
Final <i>R</i> indices ^a	<i>R</i> ₁ =0.0924,	<i>R</i> ₁ =0.1288,
[<i>I</i> >2 σ (<i>I</i>)]	<i>wR</i> ₂ =0.1986	<i>wR</i> ₂ =0.1843
<i>R</i> indices (all data)	<i>R</i> ₁ =0.0993,	<i>R</i> ₁ =0.1850,
	<i>wR</i> ₂ =0.2033	<i>wR</i> ₂ =0.2049

$$^a R_1 = \sum | |F_o| - |F_c| | / \sum |F_o|, wR_2 = \{ \sum [w(F_o^2 - F_c)^2] / \sum [w(F_o^2)^2] \}^{1/2}$$

X-ray Crystallography

X-ray single crystal diffraction data for complexes **1P** and **1M** was collected on a Bruker APEX II diffractometer at room temperature equipped with a fine focus, 2.0 kW sealed tube X-ray source (MoK radiation, $\lambda = 0.71073 \text{ \AA}$) operating at 50 kV and 30 mA. ($\lambda = 0.71073 \text{ \AA}$). The diffraction points of $I > 2\sigma(I)$ were selected to determine the structures of complex **1P** and **1M**, and solved by direct methods and refined by full-matrix least-squares methods using the SHELXS and SHELXL programs of crystallographic software package.^[19] The structures of **1P** and **1M** were solved in trigonal chiral, enantiomorphous space groups P₃₁21 (space group number 152) and P₃₂21 (space group No. 154) respectively, with correct configurations. All metal atoms, nitrogen, sulfur atoms, carbon and oxygen atoms in **1P** and **1M** were refined with anisotropic thermal parameters on *F*². All hydrogen atoms were generated geometrically (C-H 0.93 Å) and refined with isotropic thermal parameters riding on the parent atoms. The crystallographic data and structural refinement parameters for **1P** and **1M** are listed in Table 1. CCDC numbers : 1012515 for **1P** and 1012516 for **1M**.

Photocatalytic experiment

The typical process was presented as follows: 20 mg of the compound **1** was mixed together with 25 mL of 10 mg/L(C₀) RhB solution in a beaker by stirred for 2h, which makes it

reached the surface-adsorption equilibrium on the particles of the compound **1**. Then the mixture was stirred continuously under the simulated sunlight irradiation from 300W high pressure Xe lamp. At 0, 20, 40, 60, 80, 100 and 120 min. 3 mL of the sample was taken out of the beaker, respectively, then followed by several centrifugations to remove the compound **1**, and a clear solution was obtained for UV-vis analysis.

Results and discussion

Crystal Structure

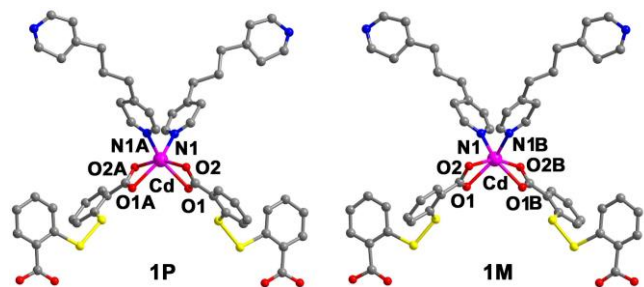


Fig. 1 The coordination environments of Cd^{2+} in **1P** and **1M**. Atoms having "A", or "B" in their labels are symmetry-generated. A: $1+x-y, -y+2, 2/3-z$; B: $y, x, -z$. Hydrogen atoms are omitted for clarity. Color code: Cd, purple; O, red; N, blue; C, grey; S, yellow.

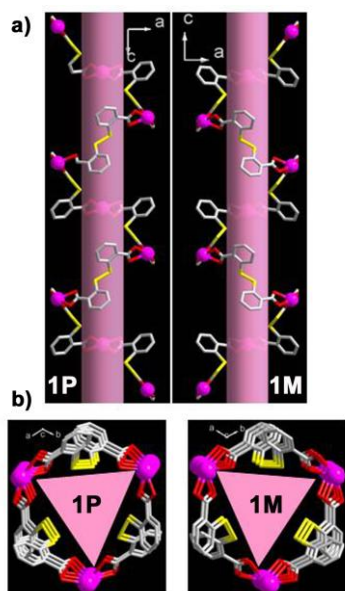


Fig. 2 (a) View of the $[\text{Cd}(\text{dtba})]$ threefold helices (right-handed in **1P**, left-handed in **1M**) running along c axis; (b) View of the triangular helical channels containing $[\text{Cd}(\text{dtba})]$ threefold helices in **1P** and **1M** along the c -axis.

Single crystallize X-ray analysis reveals that complexes $[\text{Cd}(\text{dtba})(\text{bpp})]_n$ (**1P** and **1M**) crystallize in the trigonal enantiomeric space group $P3_121$ or $P3_221$ with a flack parameter of 0.15(2) or -0.02(3), respectively, indicating enantiomeric purity of the single crystals despite the use of achiral reagents. The structures of compounds **1P** and **1M** are enantiomorphs. The asymmetric units of **1P** and **1M** both contain half Cd^{2+} ion, half of the dtba^{2-} ligand and half of bpp

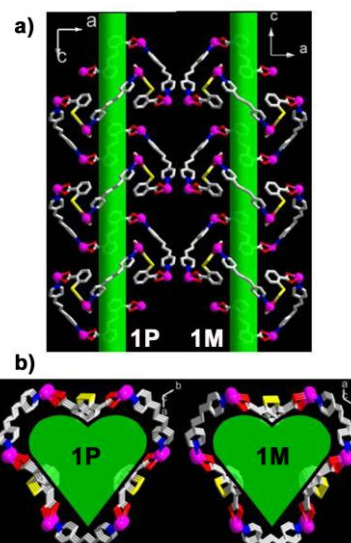


Fig. 3 (a) View of the $[\text{Cd}_2(\text{dtba})(\text{bpp})]$ threefold helices (right-handed in **1P**, left-handed in **1M**) running along c axis; (b) View of the quasi-heart-like helical channels containing $[\text{Cd}_2(\text{dtba})(\text{bpp})]$ threefold helices in **1P** and **1M** along the c -axis.

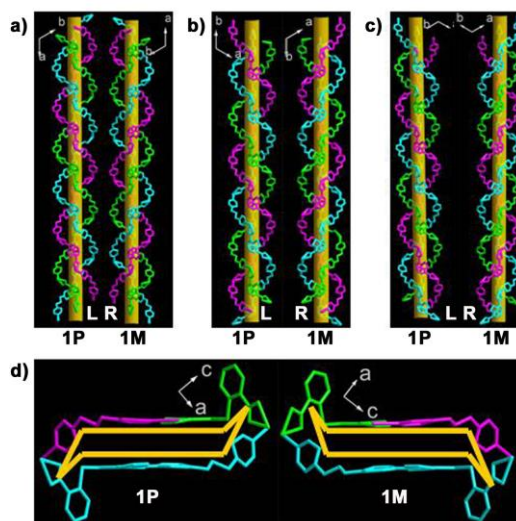


Fig. 4 View of the chair-like channels constructed from the two-fold triple-helical chains (left-handed (L) in **1P**, right-handed (R) in **1M**) running along $[100]$ direction (a), $[010]$ direction (b) and $[110]$ direction (c). The triple-helical chains are marked purple, green and cyan. (d) View of the chair-like channels along the b axis.

ligand. The six-coordinated Cd center is lying in the two-fold axis and coordinated by four carboxylic oxygen atoms of two dtba ligands and two nitrogen atoms from two bpp ligands (Fig.1) in a distorted octahedron. The lengths of Cd-O and Cd-N are in the range of 2.216(6)-2.43(3) Å and 2.283(18)-2.36(2) Å, respectively. The dtba^{2-} ligand, with a two-fold axis passing through the middle of S-S bond, adopts a twist conformation with a C-S-S-C torsion angle of ca. 86° , which can show the axial chirality with the M- and P-forms of the enantiomers to construct interesting coordination frameworks. All the carboxylate groups of dtba^{2-} ligand adopt chelating modes to connect two Cd(II) atoms (Fig.S4). The bpp molecule, with a two-

fold axis passing through C8 atom, has TT configuration and bridges two Cd(II) centers (Fig.S5).

The most interesting structure features of compounds **1P** and **1M** are the linkage between the Cd²⁺ centres and the two long flexible ligands, H₂dtba and bpp to form an unprecedented three-dimensional framework with two types of three-fold helical chiral channels, three sorts of twofold helical chiral channels and one kind of threefold double-helical chain. There are triangular and quasi-heart-like threefold helical chiral channels in **1P** and **1M** compounds. The triangular helical channels (right-handed in **1P**, left-handed in **1M**) are made of [Cd(dtba)] single helical chains formed by carboxylate group of dtba²⁻ ligands bridging Cd(II) atoms with the pitch of 16.274(2) Å (Fig 2a). The [Cd(dtba)] single helical chains wind around a threefold screw axis running parallel to the *c* axis to form a right-handed in **1P** or left-handed in **1M** helical channels with triangular shape (dimensions 10.68 × 10.68 × 10.68 Å) (Fig.2b). The quasi-heart-like threefold helical channels (right-handed in **1P**, left-handed helices in **1M**) consist of three repeating Cd-dtba–Cd-bpp linkages, in which the Cd atoms are alternatively, bridged by dtba²⁻ and bpp ligands with the pitch of 16.274(2) Å (Fig 3). In addition, there are similar chair-like twofold helical chiral channels with the reverse helical orientation to threefold helical chiral channels (left-handed in **1P**, right-handed helices in **1M**) running parallel to the [100], [010] and [110] three directions, respectively (Fig 4). The three types of chair-like helical channels are all constructed from the triple-helical chains. The separations between the adjacent helical chains are the same as the length of the *a* or *b* axis (11.730(1) Å). The pitch of the chair-like helical channels are three times the length of *a* or *b* axis. The triple-helical chains are made of two repeating Cd-dtba–Cd-bpp linkages running parallel to the twofold screw axes.

helical orientation as the chair-like twofold helical channels (left-handed in **1P**, right-handed helices in **1M**) with the pitch of twice as the length of the *c* axis running along the threefold screw axis. The separation between the two equivalent Cd-bpp helical chains is the same as the length of the *c* axis (Fig 5). The two equivalent Cd-bpp helical chains strand spiral parallel around a threefold screw axis to generate double-helical chains. The double-helical chains overlap and look like flowers with three petals as viewed from the *c* axis. The double-helical chains as pillars are connected by the dtba²⁻ ligands *via* Cd-O interactions to produce a 3D open-framework, exhibiting different helical chiral channels (Fig 6a, 6b). The large porosity of **1P** and **1M** allows the interpenetration of the network by other independent network. In **1P** and **1M**, there are three interpenetrated nets, which are related by the translation vector of *a* (11.730(1) Å), so **1P** and **1M** are threefold interpenetrated 3D chiral frameworks (Fig 6c).

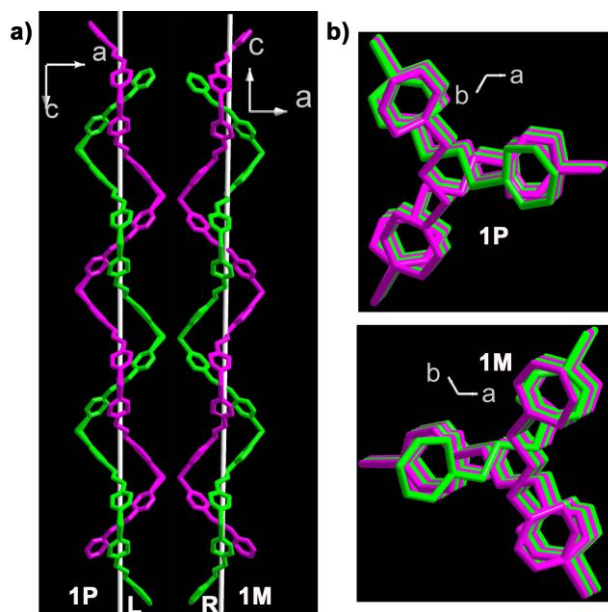


Fig. 5 (a) The threefold [Cd(bpp)]_n double-stranded helices (left-handed (L) in **1P**, right-handed (R) in **1M**) viewed upright to the *c* axis. The double helical chains are marked purple, and green. (b) View of the threefold double-stranded helices along the *c* axis.

Remarkably, bpp ligands with the TT configuration bridge Cd²⁺ centres to form two equivalent Cd-bpp helical chains with the same

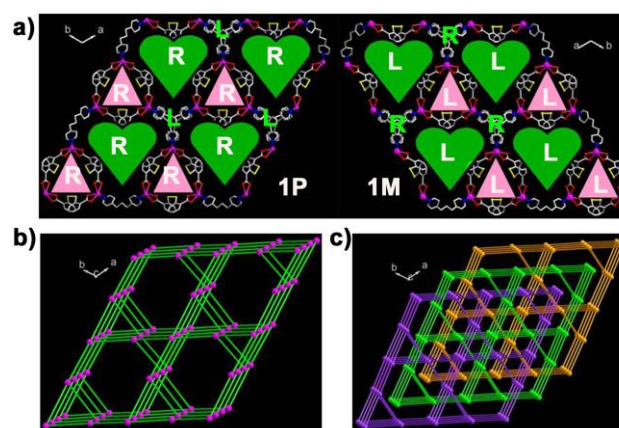


Fig. 6 (a) The 3D frameworks of **1P** and **1M** viewed along the *c* axis, showing triangular and quasi-heart-like threefold helical chiral channels in **1P** and **1M** and double-helical chains. L and R indicate the left- and right-handed helical channels; (b) A single 8⁶ network in **1P** viewed close along the *c* axis. (c) Three interpenetrating 8⁶ nets (purple, green and orange) in **1P** viewed along the *c* axis.

Topologically, the 3D metal-organic framework of **1** can be regarded as a uninodal four-connected *bcu*-topology net taking the Cd²⁺ ions as four-connected nodes. The Schläfli symbol for the four-connected uniform networked is 8⁶, which is calculated in TOPOS 4.0(Fig 6b). The extended point symbol is [8⁶.8⁶.8⁷.8⁷.8⁷]. Interestingly, the compounds **1P** and **1M** crystallize in the chiral space P3₁21(No.152) or P3₂21(No.154). Therefore, compounds **1P** and **1M** show chiral threefold interpenetrating 4-connected 8⁶ network, which are rarely reported.

XRD, IR spectra and UV spectra analyses

As shown in Fig.S6, the good accordance of experimental XRD patterns with the simulated patterns indicates phase purity of compound **1**.

The IR spectrum (Fig.S3) of **1** exhibits strong and sharp absorption peaks of 1573 and 1398 cm⁻¹ associated with the ν_{asym}(C=O) and ν_{sym}(C=O), respectively, and also peaks at 860 and 746 cm⁻¹ corresponding to the ν_s(S-S) of the dtba²⁻ ligand.

The UV-vis absorption spectrum was performed at room temperature for **1**. Absorption data R/S (R, absorption coefficient; S, scattering factor) was calculated from the

reflectance data using the Kubelka-Munk function. The optical band gap of 2.92 eV (the a point in Fig. S7) was measured as the intersection point between the energy axis at the absorption offset and the line extrapolated from the sharp absorption edge in the K-M versus E (eV) plot [20]. The optical band gap indicates that compound **1** is a semiconducting MOF, underlining its potential as a photocatalyst.

The chiroptical characteristics of compound **1** by CD spectra

Circular dichroism (CD) spectroscopy is the most common techniques for characterizing the optical activity of chiral materials. In order to confirm the compounds **1P** and **1M** enantiomeric nature, the individual crystals were characterized by solid-state circular dichroism (CD) spectroscopy in KCl pellet (Fig.7). As shown in Fig. 7, the CD spectra of enantiomers are nearly mirror images of each other, indicating the enantiomeric nature of the compounds. The signal of purple curve (**1P**) and orange curve (**1M**) can be observed obvious cotton effect. The purple curve showed three positive peaks at 220 nm, 267 nm and 317 nm, as well as one negative peak at 243 nm, which may be considered as the signature of the **1P** helicity. However, opposite signals at the same wavelengths for compound **1** are observed too, showing only one strong positive peaks at 247 nm, and two negative peaks at 221nm and 320 nm corresponding to **1M**. There is no dichroism signals in a mixture of a few crystals. Concurrence of the CD experiments and single-crystal studies confirms that the sample is a conglomerate consisting of enantiomorphs **1P** and **1M**, which confirms spontaneous resolution during the course of crystallization.

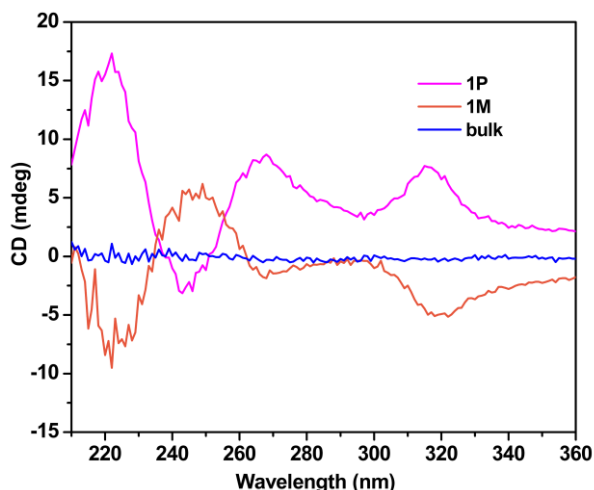


Fig. 7 Solid-state CD spectra of **1P** (purple), an enantiomorph **1M** (red), and a mixture of a few crystals (blue).

Thermal properties

Thermal analysis was carried out from 30 °C to 1000 °C for **1** under the nitrogen atmosphere (Fig.S8). Because there are not any solvent molecules in **1**, compound **1** is stable up to 280 °C, the first weight loss of 50.68 % (calcd, 49.82 %) in the temperature of 280-370 °C can be assigned to the decomposition

of dtba²⁻ ligand. The second weight loss of 16.93 % (calcd, 16.12%) in the range of 370-470 °C corresponds to the removal of the organic bpp ligand. The remaining weight is attributed to the formation of CdO (obsd,17.89 %; calcd,20.88 %) and the slow evaporation of CdO.

Photoluminescence property

The photoluminescence properties of **1** and H₂dtba ligand were investigated in the solid state at room temperature. As shown in Fig.8, upon excitation at 360 nm, the compound **1** displays a blue luminescence with a peak maximum at 465 nm. Compared with the emission spectra of H₂dtba at 452 nm (λ_{ex} =398 nm) and bpp at 455 nm (λ_{ex} =360 nm)^[13b] red shifts of 13 nm and 10 nm in **1** were observed (Fig 8). This may be attributed to the cooperative effect of the neutral bpp ligand and the carboxylate ligands. As a result, the emission can be assigned to intraligand fluorescence^[13b]. It suggests that compound **1** might be a good candidate as photoactive material.

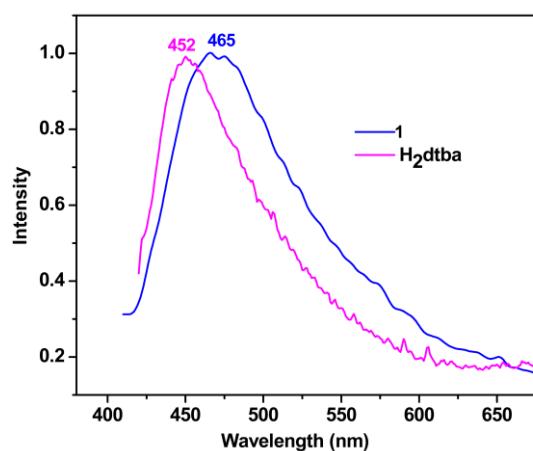


Fig. 8 Emission spectrum for solid compound **1** (λ_{ex} =360 nm) and H₂dtba (λ_{ex} =398 nm) at room temperature

Photocatalytic property

To investigate the photocatalytic activity of compound **1** as catalyst, the photodecomposition of Rhodamine-B (RhB) in aqueous solution is evaluated under the simulated sunlight irradiation. To explore the optimum conditions of photocatalytic activity, the degradation processes of RhB were studied using the same photocatalyst in different pH solutions. The different pH comparative experiments were made to investigate the photocatalytic activity of compound **1** under identical conditions. It is the first time to investigate photocatalytic activity of MOFs in different pH solutions. The pH values of RhB solution were adjusted to 1, 3, 5, 7 and 10 by adding HCl or NaOH solution.

The characteristic absorption band of RhB at 554 nm was used to monitor the degradation process as a function of irradiation time. Fig 9 and Fig.S9-S12 show the temporal evolution of the absorption spectra of the RhB solution degraded by compound **1** at different pH value under the simulated sunlight irradiation. The decomposition rate of RhB (K) can be expressed as K =

$(I_0 - I_t)/I_0$, where I_0 presents the *UV-vis* absorption intensity of RhB at the initial time ($t=0$) and the I_t is the intensity at a given

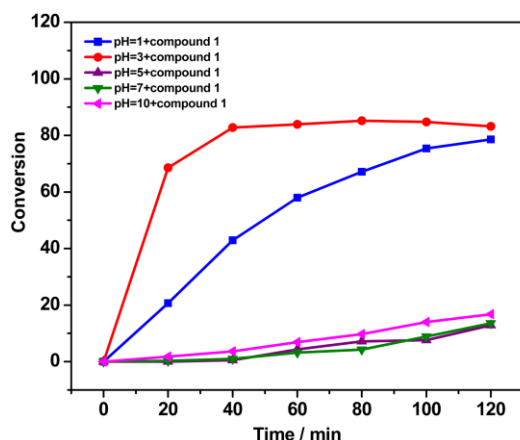


Fig. 9 Conversion rate of RhB (K) with the reaction time (t) in different pH value solution with compound 1.

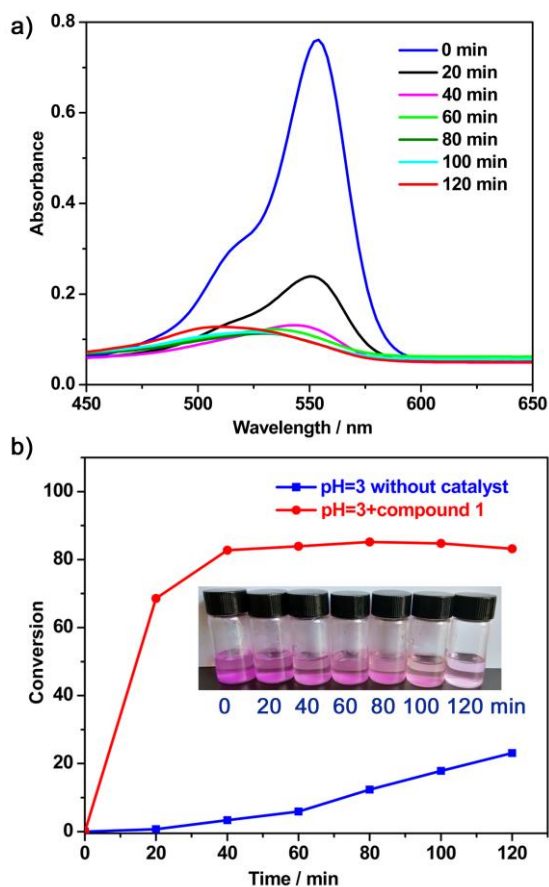


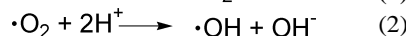
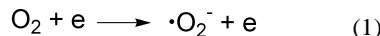
Fig. 10 (a) Absorption spectra of the RhB aqueous solution with pH=3 during the photodegradation under 300 W high pressure Xe lamp irradiation with compound 1; (b) Conversion rate of RhB (K) with the reaction time (t) with compound 1 and without catalyst in the pH=3 solution.

time (t). When the pH value of the RhB solution is 1, 3, 5, 7 and 10, it is found that the maximum absorbance at 554 nm of the blank RhB aqueous solution decreases from 1.60 to 0.96, 2.00 to 1.55, 1.99 to 1.81, 2.40 to 2.22, and 2.40 to 2.23

respectively, after the 120-min simulated sunlight irradiation while those in the presence of **1** decrease from 0.93 to 0.17, 0.76 to 0.09, 1.95 to 1.70, 2.35 to 2.03, 2.38 to 1.98, respectively, after the same time the simulated sunlight irradiation. On the basis of the experimental results, the decomposition rate of RhB without catalyst and with compound **1** reach 41% and 78% at pH =1, 23% and 85% at pH =3, 9% and 13% at pH =5, 7% and 13% at pH =7, 7% and 17% at pH =10 (120-min the simulated sunlight irradiation) (Fig.9 and S13), respectively. Figures of S10-S12 present the *UV-vis* absorption spectra of RhB at different pH values under the simulated sunlight irradiation. It is found that the absorption spectra of RhB remain unchanged obviously with acid, neutral, and basic solution and it also means the conjugated structure of RhB does not be decomposed at different pH values. These results demonstrate that the use of **1** can dramatically accelerate the photodegradation reaction of RhB in aqueous solutions. These experiments also reveal that the pH values of the solution play a key role in the photodecomposition of RhB. When the compound **1** was used in the pH =3 RhB solution, the absorption peak of the dye undergoes a fairly large decrease, and the hypsochromic shifts of the absorption band are considerably insignificant (Fig 10). It is presumed that the compound **1** at pH=3 showed the best photocatalytic activity in RhB degradation.

In addition, during the course of the photocatalytic reactions, the photostability of compound **1** was monitored using PXRD patterns. The PXRD patterns are in good agreement with that of the original compound implying that **1** maintains its structural integrity after the photocatalysis reaction, which confirmed that its stability towards photocatalysis is good (Fig. S14).

The possible photocatalytic mechanism^[21] for the above degradation reactions is proposed as follows (Scheme S1). Upon irradiation using the simulated sunlight light, because the absorption of energy equal to or greater than the band gap of **1** (Fig. S7 $h\nu \cong 2.92\text{eV}$), electrons (e^-) in the valence band (VB) are excited to the conduction band (CB), leaving the same amount of holes (h^+) in the VB. Electrons (e^-) have reducing and holes (h^+) have oxidation. The electrons reduce the oxygen (O_2) to oxygen radicals ($\cdot\text{O}_2^-$), and finally they may turn into hydroxyl radicals ($\cdot\text{OH}$) by the combination of H^+ cations. At the same time, holes oxidize the hydroxyl (H_2O) to hydroxyl radical ($\cdot\text{OH}$). Such a hydroxyl radical ($\cdot\text{OH}$) is known to have high activity to decompose the organic dyes, such as RhB^[22].



The dissolved O_2 in a aqueous solution, as an efficient electron trap, leads to the generation of hydroxyl radical ($\cdot\text{OH}$), thus preventing the recombination of electrons and holes. According to the Eqs, (1) and (2), the addition of HCl will be favorable for the formation of hydroxyl radical ($\cdot\text{OH}$). As a result, the conversion rate of RhB is improved by the addition of acid. Our research demonstrates that the high photocatalytic activity is achieved under the acidic condition (pH = 1 and 3), especially,

compound **1** at pH=3 showed the best photocatalytic activity in RhB degradation.

Conclusion

In summary, we have successfully constructed two 3D three-interpenetrating chiral cadmium MOF enantiomers by spontaneous resolution upon crystallization without chiral resource. Interestingly, the structure of **1** consists two types of threefold helical chiral channels (triangular and quasi-heart-like chiral channels), three sorts of twofold helical chiral channels (chair-like chiral channel) and one kind of threefold double-helical chains. The compounds **1P** and **1M** are optically active, and their CD spectra show Cotton effects in the opposite direction. Photocatalytic activity studies reveal that compound **1** at pH=3 shows the best photocatalytic activity in RhB degradation. It is the first time to investigate photocatalytic activity of MOFs in different pH solutions.

Acknowledgements

This work was supported by the National Natural Science Foundation of China (Grant. 21473030 and 21003020), the Natural Science Fund of Fujian Province (Grant. 2013J01041) and the Foundation of State Key Laboratory of Structural Chemistry (Grant. 20130012).

Reference

- (a) B. Panella, M. Hirscher, H. Putter and U. Muller, *Adv. Funct. Mater.*, 2006, **16**, 520; (b) D. Q. Yuan, W. G. Lu, D. Zhao and H. C. Zhou, *Adv. Mater.*, 2011, **23**, 3723; (c) S. Q. Ma, X. S. Wang, D. Q. Yuan and H. C. Zhou, *Angew. Chem., Int. Ed.*, 2008, **47**, 4130; (d) X. S. Wang, S. Q. Ma, P. M. Forster, D. Q. Yuan, J. Eckert, J. J. Lopez, B. J. Murphy, J. B. Parise and H. C. Zhou *Angew. Chem., Int. Ed.*, 2008, **47**, 7263; (e) D. Yuan, D. Zhao, D. F. Sun and H. C. Zhou, *Angew. Chem., Int. Ed.*, 2010, **49**, 5357; (f) T. Fukushima, S. Horike, Y. Inubushi, K. Nakagawa, Y. Kubota, M. Takata and S. Kitagawa, *Angew. Chem. Int. Ed.*, 2010, **49**, 4820; (g) R. Vaidhyanathan, S. S. Iremonger, G. K. H. Shimizu, P. G. Boyd, S. Alavi and T. K. Woo, *Angew. Chem. Int. Ed.*, 2012, **51**, 1826; (h) R. B. Getman, Y. S. Bae, C. E. Wilmer and R. Q. Snurr, *Chem. Rev.*, 2012, **112**, 703; (i) M. P. Suh, H. J. Park, T. K. Prasad and D. W. Lim, *Chem. Rev.*, 2012, **112**, 782; (j) K. Sumida, D. L. Rogow, J. A. Mason, T. M. McDonald, E. D. Bloch, Z. R. Herm, T. H. Bae and J. R. Long, *Chem. Rev.*, 2012, **112**, 724.
- (a) W. G. Lu, J. P. Sculley, D. Q. Yuan, R. Krishna, Z. W. Wei and H. C. Zhou, *Angew. Chem. Int. Ed.*, 2012, **51**, 7480-7484; (b) W. G. Lu, D. Q. Yuan, D. Zhao, C. I. Schilling, O. Plietsch, T. Muller, S. Brase, J. Guenther, J. Blumel, R. Krishna, Z. Li and H. C. Zhou, *Chem. Mater.*, 2010, **22**, 5964.
- (a) S. Q. Ma, D. F. Sun, X. S. Wang and H. C. Zhou, *Angew. Chem., Int. Ed.*, 2007, **46**, 2458; (b) J. R. Li, R. J. Kuppler and H. C. Zhou, *Chem. Soc. Rev.*, 2009, **38**, 1477; (c) M. C. Das, Q. S. Guo, Y. B. He, J. Kim, C. G. Zhao, K. L. Hong, S. C. Xiang, Z. J. Zhang, K. M. Thomas, R. Krishna and B. L. Chen, *J. Am. Chem. Soc.*, 2012, **134**, 8703; (d) S. Horike, K. Kishida, Y. Watanabe, Y. Inubushi, D. Umeyama, M. Sugimoto, T. Fukushima, M. Inukai and S. Kitagawa, *J. Am. Chem. Soc.*, 2012, **134**, 9852.
- (a) P. F. Shi, G. Xiong, B. Zhao, Z. Y. Zhang and P. Cheng, *ChemComm.*, 2013, **49**, 2338; (b) J. J. Zhang, S. Q. Xia, T. L. Sheng, S. M. Hu, G. Leibeling, F. Meyer, X. T. Wu, S. C. Xiang and R. B. Fu, *ChemComm.*, 2004, 1186; (c) X. F. Li, Y. B. Huang and R. Cao, *Cryst Growth & Des.*, 2012, **12**, 3549; (d) L. Liang, G. Peng, L. Ma, L. Sun, H. Deng, H. Li and W. S. Li, *Cryst Growth & Des.*, 2012, **12**, 1151; (e) J. J. Zhang, S. M. Hu, S. C. Xiang, T. L. Sheng, X. T. Wu and Y. M. Li, *Inorg. Chem.*, 2006, **45**, 7173 (f) J. W. Cheng, S. T. Zheng, E. Ma and G. Y. Yang, *Inorg. Chem.*, 2007, **46**, 10534.
- Y. Zhu, F. Luo, Y. M. Song, X. F. Feng, M. B. Luo, Z. W. Liao, G. M. Sun, X. Z. Tian and Z. J. Yuan, *Cryst Growth & Des.*, 2012, **12**, 2158.
- (a) H. Y. Xu, F. H. Zhao, Y. X. Che and J. M. Zheng, *CrystEngComm*, 2012, **14**, 6869; (b) V. Chandrasekhar, B. M. Pandian, J. J. Vittal and R. Clerac, *Inorg. Chem.*, 2009, **48**, 1148; (c) V. Gomez, L. Vendier, M. Corbella and J. P. Costes, *Inorg. Chem.*, 2012, **51**, 6396; (d) Y. Liu, Z. Chen, J. Ren, X. Q. Zhao, P. Cheng and B. Zhao, *Inorg. Chem.*, 2012, **51**, 7433.
- Q. Yue, J. Yang, G. H. Li, G. D. Li, W. Xu, J. S. Chen and S. N. Wang, *Inorg. Chem.*, 2005, **44**, 5241.
- G. F. Xu, P. Gamez, J. K. Tang, R. Clerac, Y. N. Guo and Y. Guo, *Inorg. Chem.*, 2012, **51**, 5693.
- (a) Z. Y. Li, J. Zhu, X. Q. Wang, J. Ni, J. J. Zhang, S. Q. Liu and C. Y. Duan, *Dalton Trans.*, 2013, **42**, 5711; (b) V. Chandrasekhar, B. M. Pandian, R. Boomishankar, A. Steiner, J. J. Vittal, A. Hourri and R. Clerac, *Inorg. Chem.*, 2008, **47**, 4918; (c) Y. Ouyang, W. Zhang, N. Xu, G. F. Xu, D. Z. Liao, K. Yoshimura, S. P. Yan and P. Cheng, *Inorg. Chem.*, 2007, **46**, 8454; (d) E. Colacio, J. Ruiz, A. J. Mota, M. A. Palacios, E. Cremades, E. Ruiz, F. J. White and E. K. Brechin, *Inorg. Chem.*, 2012, **51**, 5857; (e) A. Jana, S. Majumder, L. Carrella, M. Nayak, T. Weyhermueller, S. Dutta, D. Schollmeyer, E. Rentschler, R. Koner and S. Mohanta, *Inorg. Chem.*, 2010, **49**, 9012.
- (a) B. Zhao, X. Y. Chen, Z. Chen, W. Shi, P. Cheng, S. P. Yan and D. Z. Liao, *ChemCommun.*, 2009, 3113; (b) G. Peng, G. E. Kostakis, Y. H. Lan and A. K. Powell, *Dalton Trans.*, 2013, **42**, 46; (c) G. M. Li, T. Akitsu, O. Sato and Y. Einaga, *J. Am. Chem. Soc.*, 2003, **125**, 12396.
- (a) G. B. Deacon and R. J. Phillips, *Coord. Chem. Rev.*, 1980, **33**, 227; (b) K. K. Bisht and E. Suresh, *J. Am. Chem. Soc.*, 2013, **135**, 15690; (c) K. K. Bisht and E. Suresh, *Inorg. Chem.* 2012, **51**, 9577; (d) A. Kaur, G. Hundal and M. S. Hundal, *Cryst. Growth. Des.*, 2013, **13**, 3996.
- (a) R. Vaidhyanathan, S. Natarajan and C. N. R. Rao, *Inorg. Chem.* 2002, **41**, 5226; (b) H. Wang, Z. Chang, Y. Li, R. M. Wen and X. H. Bu, *Chem. Commun.*, 2013, **49**, 6659; (c) L. M. Zhang, D. Y. Deng, G. Peng, L. Sun, L. Liang, G. Q. Lan and H. Deng, *CrystEngComm.*, 2012, **14**, 8083; (d) Z. Su, M. S. Chen, J. Fan, M. Chen, S. S. Chen, L. Luo and W. Y. Sun, *CrystEngComm.*, 2012, **14**, 2040.
- (a) Y. Bu, F. L. Jiang, S. Q. Zhang, J. Ma, X. J. Li and M. C. Hong, *CrystEngComm*, 2013, **13**, 6323; (b) R. Feng, F. L. Jiang, L. Chen, C. F. Yan, M. Y. Wu and M. C. Hong, *ChemComm.*, 2009, 5296; (c) Y. F. Hou, Y. Yu, K. F. Yue, Q. Wei, Y. L. Liu, C. S. Zhou and Y. Y. Wang, *CrystEngComm*, 2013, **15**, 7161; (d) M. Hu, S. T. Ma, L. Q. Guo, L. M. Zhou, L. J. Gao, S. M. Fang and C. S. Liu, *Z. Anorg. Allg. Chem.*, 2010, **636**, 616.
- (a) L. H. Cao, Y. L. Wei, Y. Yang, H. Xu, S. Q. Zang, H. W. Hou and T. C. W. Mak, *Crystal. Growth. Des.*, 2014, **14**, 1827; (b) L. Han, H. Valle and

- X.H. Bu, *Inorg. Chem.*, 2007, **46**, 1511; (c) Z. H. Li, L. P. Xue, S. H. Li, J. G. Wang, B. T. Zhao, J. Kan and W. P. Su, *CrystEngComm*, 2013, **15**, 2745; (d) J. C. Jin, Y. N. Zhang, Y. Y. Wang, J. Q. Liu, Z. Dong and Q. Z. Shi, *Chem. Asian J.*, 2010, **5**, 1611.
- 15 (a) Y. Q. Zheng, J. Zhang and J. Y. Liu, *CrystEngComm*, 2010, **12**, 2740; (b) B. Murugesapandian and P. W. Roesky, *Inorg. Chem.*, 2011, **50**, 1698; (c) F. L. Hu, W. Wu, P. Liang, Y. Q. Gu, L. G. Zhu, H. Wei and J. P. Lang, *Crystal. Growth. Des.*, 2013, **13**, 5050; (d) Q. Sun, Y. Q. Wang, A. L. Cheng, K. Wang and E. Q. Gao, *Crystal. Growth. Des.*, 2012, **12**, 2234; (e) W. H. Zhang, Y. L. Song, Z. H. Wei, L. L. Li, Y. J. Huang, Y. Zhang and J. P. Lang, *Inorg. Chem.*, 2008, **47**, 5332.
- 16 (a) D. Sun, F. J. Liu, R.-B. Huang and L. S. Zheng, *Inorg. Chem.*, 2011, **50**, 12393-12395; (b) S. M. Humphrey, R. A. Mole, J. M. Rawson and P. T. Wood, *Dalton. Trans.*, 2004, 1670.
- 17 L. Carlucci, G. Ciani, D. M. Proserpio and S. Rizzato, *CrystEngComm*, 2002, **4**, 121.
18. (a) Y. Q. Sun, J. Zhang, Y. M. Chen and G. Y. Yang, *Angew. Chem. Int. Ed.*, 2005, **44**, 5814; (b) Y. Q. Sun, J. Zhang and G. Y. Yang, *Chem. Comm.*, 2006, 1947; (c) Y. Q. Sun, J. Zhang and G. Y. Yang, *Chem. Comm.*, 2006, 4700.
- 19 (a) G. M. Sheldrick, *SHELXS-97, Program for X-ray Crystal Structure Solution*; University of Göttingen: Göttingen, Germany, 1997; (b) G. M. Sheldrick, *SHELXL-97, Program for X-ray Crystal Structure Refinement*; University of Göttingen: Göttingen, Germany, 1997.
- 20 (a) J. Li, Z. Chen, X. Wang and D. M. Proserpio, *J. Alloy. Compd.*, **1997**, 262–263, 28–33; (b) A. Mesbah, S. Lebègue, J. M. Klingsporn, W. Stojko, R. P. Van Duyne and J. A. Ibers, *J. Solid. State. Chem.*, 2013, **200**, 349–353; (c) T.-H. Bang, S.-H. Choe, B.-N. Park, M.-S. Jin and W.-T. Kim, *Semicond. Sci. Tech.*, 1996, **11**, 1159; (d) Y. Q. Sun, S. Z. Ge, Q. Liu, J. C. Zhong, Y. P. Chen, *CrystEngComm.*, 2013, **15**, 10188.
- 21 (a) M. C. Das, H. Xu, Z. Wang, G. Srinivas, W. Zhou, Y. F. Yue, V. N. Nesterov, G. Qian and B. Chen, *ChemComm.*, 2011, 47, 11715; (b) T. Wen, D. X. Zhang and J. Zhang, *Inorg. Chem.*, 2013, **52**, 12; (c) F. Wang, Z. S. Liu, H. Yang, Y. X. Tan and J. Zhang, *Angew. Chem. Int. Ed.*, 2011, **50**, 450; (d) L. Liu, J. Ding, C. Huang, M. Li, H. Hou, and Y. Fan, *Crystal. Growth. Des.*, 2014, **14**, 3035.
- 22 (a) C. Galindo, P. Jacques and A. Kalt, *J. Photochem. Photobiol.*, A, 2000, **130**, 35; (b) J. Joseph, H. Destailats, H. Hung and M. Hoffmann, *J. Phys. Chem. A*, 2000, **104**, 301–307.